Neuron
Article

Dynamic Sensory Representations in the Olfactory Bulb: Modulation by Wakefulness and Experience

Hiroyuki K. Kato,[1,4] Monica W. Chu,[1,2,4] Jeffry S. Isaacson,[1,*] and Takaki Komiyama[1,2,3,*]
[1]Center for Neural Circuits and Behavior and Department of Neurosciences
[2]Neurobiology Section, Division of Biological Sciences
[3]JST, PRESTO
University of California, San Diego, La Jolla, CA 92093, USA
[4]These authors contributed equally to this work
*Correspondence: jisaacson@ucsd.edu (J.S.I.), tkomiyama@ucsd.edu (T.K.)
http://dx.doi.org/10.1016/j.neuron.2012.09.037

SUMMARY

How are sensory representations in the brain influenced by the state of an animal? Here we use chronic two-photon calcium imaging to explore how wakefulness and experience shape odor representations in the mouse olfactory bulb. Comparing the awake and anesthetized state, we show that wakefulness greatly enhances the activity of inhibitory granule cells and makes principal mitral cell odor responses more sparse and temporally dynamic. In awake mice, brief repeated odor experience leads to a gradual and long-lasting (months) weakening of mitral cell odor representations. This mitral cell plasticity is odor specific, recovers gradually over months, and can be repeated with different odors. Furthermore, the expression of this experience-dependent plasticity is prevented by anesthesia. Together, our results demonstrate the dynamic nature of mitral cell odor representations in awake animals, which is constantly shaped by recent odor experience.

INTRODUCTION

Interpreting and acting upon incoming sensory information in contextually appropriate ways is crucial for the survival of an animal. Revealing how sensory representations in the brain are affected by factors such as brain state and the animal's history is an important step toward understanding how the brain processes sensory information. Here we address this issue by exploring how the intial stages of olfactory information processing are modulated by wakefulness and experience.

Odors are detected by odorant receptors on olfactory sensory neurons (OSNs), each of which expresses one of ~1,000 odorant receptors (Buck and Axel, 1991). The axons of OSNs expressing the same receptor converge onto one to two glomeruli in the olfactory bulb (Mombaerts et al., 1996), where different odors activate distinct sets of glomeruli (Belluscio and Katz, 2001; Bozza et al., 2004; Igarashi and Mori, 2005; Johnson et al., 2005; Onoda, 1992; Rubin and Katz, 1999; Soucy et al., 2009; Stewart et al., 1979; Wachowiak and Cohen, 2001; Xu et al., 2000, 2003; Yang et al., 1998). Within glomeruli, odor information is relayed to mitral cells, the major output neurons of the bulb. Mitral cells send their apical dendrites to a single glomerulus and thus receive direct input from OSNs expressing a single odorant receptor type (Wilson and Mainen, 2006). The activity of mitral cells is thought to be modulated by local inhibitory interneurons (Arevian et al., 2008; Isaacson and Strowbridge, 1998; Schoppa et al., 1998; Schoppa and Urban, 2003; Urban and Arevian, 2009; Wilson and Mainen, 2006; Yokoi et al., 1995) (Figure 1A).

Previous studies have examined mitral cell odor representations, mainly using acute recordings in anesthetized rodents. These studies showed that odors activate distinct ensembles of mitral cells (Bathellier et al., 2008; Davison and Katz, 2007; Dhawale et al., 2010; Fantana et al., 2008; Meredith, 1986; Mori et al., 1992; Tan et al., 2010). Less is known, however, about mitral cell activity in awake animals, which appears to be different from the anesthetized state (Adrian, 1950; Rinberg et al., 2006b) and can depend on the behavioral context (Doucette et al., 2011; Doucette and Restrepo, 2008; Kay and Laurent, 1999).

In this study, we address several important questions regarding odor coding in the mammalian olfactory bulb. First, how does odor coding by mitral cell ensembles depend on brain state? Accumulating evidence suggests that odor coding in the olfactory bulb relies on temporally dynamic population activity (Bathellier et al., 2008; Friedrich and Laurent, 2001; Stopfer et al., 1997). Therefore, it is important to understand how brain state regulates odor-evoked activity patterns of neural ensembles over time. Second, how is the activity of inhibitory interneurons in the bulb modulated by brain state? Granule cells are a major class of GABAergic interneurons in the olfactory bulb that mediate mitral cell recurrent and lateral inhibition (Isaacson and Strowbridge, 1998; Schoppa et al., 1998; Yokoi et al., 1995). However, in vivo recordings of their activity have been limited to a few studies in anesthetized animals (Cang and Isaacson, 2003; Tan et al., 2010). Lastly, how does odor experience shape odor coding over long periods of time (days to months) in awake animals? Previous studies have established that even passive

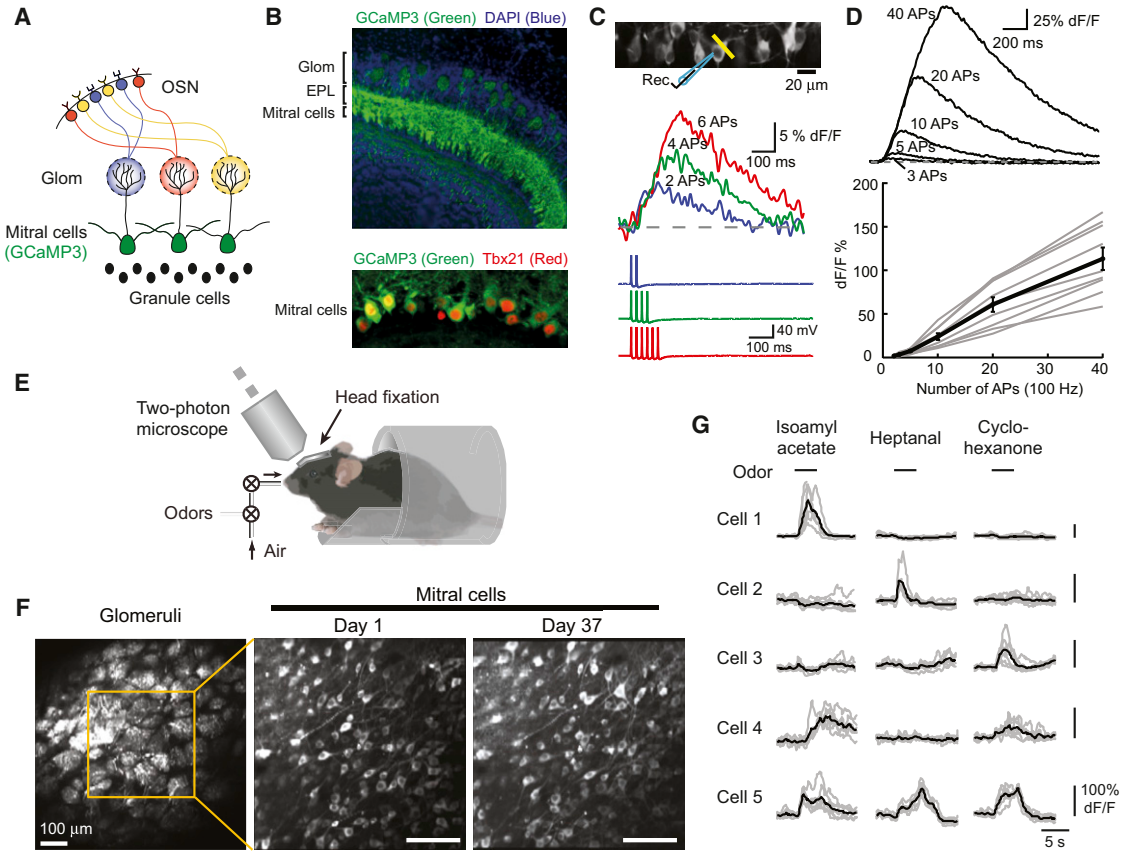

Figure 1. Long-Term Imaging of Mitral Cell Activity in Awake Mice

(A) Olfactory bulb schematic. OSN, olfactory sensory neurons; Glom, glomeruli. Each color represents OSNs that express a unique odorant receptor.

(B) Top: fixed thin section of the dorsal olfactory bulb 4 weeks after injection of AAV-hSyn-FLEX-GCaMP3 into the olfactory bulb of a PCdh21-Cre mouse. Note the dense labeling in the mitral cell layer. All glomeruli in the field of view contain apical dendrites of mitral cells expressing GCaMP3. GCaMP3 fluorescence in the external plexiform layer (EPL) largely reflects dendrites of mitral cells with additional contributions from tufted cells, which also express Cre. GCaMP3 fluorescence in deeper bulb layers represents expression in mitral cell axons. Bottom: expression of GCaMP3 in the mitral cell layer colocalizes with immunolabeling of Tbx21, a mitral cell-specific marker.

(C) Top: two-photon single plane image of the mitral cell layer in an olfactory bulb slice from a GCaMP3-expressing PCdh21-Cre mouse illustrating recording configuration and region of line scan (yellow). Bottom: average fluorescence transients (three trials) evoked by two, four, and six action potentials (APs) at 50 Hz (1 nA, 3 ms current steps) in the same cell.

(D) Top: average GCaMP3 responses (two to five trials) from a representative cell in response to a range of APs elicited at 100 Hz . Bottom: summary of the increase in dF/F (n = 9 cells) for varying numbers of APs elicited at 100 Hz indicates that GCaMP3 is a relatively linear reporter of AP firing. Black line represents average response and gray lines represent responses of individual cells. Error bars represent SEM in this and all subsequent figures.

(E) In vivo imaging configuration.

(F) Two-photon imaging of GCaMP3-expressing mitral cells in vivo. Left: imaging ~50 µm under pial surface in the glomerular layer shows that all glomeruli (~60) in the field of view contain GCaMP3-expressing dendrites. Middle: imaging ~200 µm deeper in the mitral cell layer (zoomed in from the yellow square on the left) reveals ~100 GCaMP3-expressing mitral cell somata. Right: the same sets of mitral cells imaged 37 days later.

(G) Different odors activate overlapping but distinct ensembles of simultaneously imaged mitral cells. Gray, seven individual trials; black, average trace.

odor exposure can modify mitral cell activity (Buonviso and Chaput, 2000; Buonviso et al., 1998; Chaudhury et al., 2010; Fletcher and Wilson, 2003; Spors and Grinvald, 2002; Wilson, 2000; Wilson and Linster, 2008). However, these studies mainly focused on acute recordings in anesthetized rodents and the long-term effects of experience on odor representations in awake animals are unclear.

These questions have been difficult to address, partly because of the challenge of recording from large ensembles of neurons of an identified cell type over long time periods in awake animals. Here we overcome this challenge by using chronic two-photon calcium imaging with the genetically encoded calcium indicator GCaMP3. By selectively imaging the activity of ensembles of mitral cells and inhibitory granule cells, we show that the transition from the awake to anesthetized brain state modulates olfactory bulb circuits and odor coding. Furthermore, we monitored the dynamics of odor responses of the same populations of mitral cells over months in awake mice to test how odor experience affects olfactory bulb odor representations. These approaches revealed a surprisingly dynamic nature of odor representations, which is sensitive to brain state and experience.

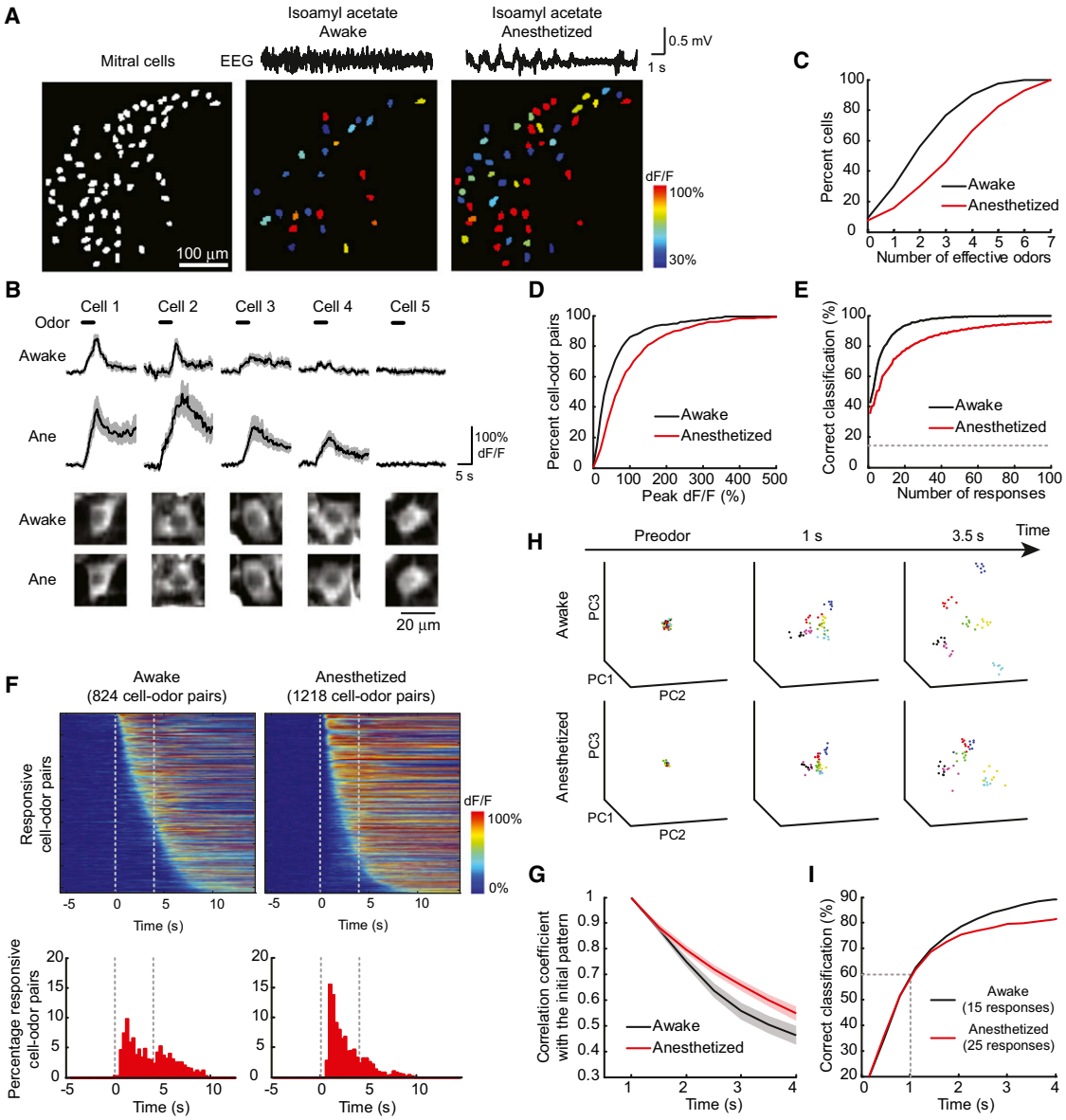

Figure 2. Mitral Cell Odor Responses in the Awake State Are More Sparse, Temporally Dynamic, and Efficient Compared to the Anesthesized Brain State

(A) Mitral cell odor-evoked activity maps (pseudocoloring represents odor-evoked GCaMP3 dF/F response averaged across seven trials) from a mouse recorded before and after the induction of anesthesia. Mitral cell ensemble response is weaker in the awake state (middle) compared to the anesthestized state (right). The left panel shows all imaged mitral cells in white. The top traces show example EEG traces during both states.

(B) Average (solid lines) and SEM (shading) of odor-evoked GCaMP3 responses from five mitral cells in (A) during awake and anesthesized states show an increase in odor-evoked activity after the induction of anesthesia. Images at the bottom show that each mitral cell was clearly identified under both conditions.

(C) Summary data shown in cumulative frequency plot of odor tuning (the number of odors eliciting responses out of the seven tested odors) for 340 mitral cells in the awake state compared to after induction of anesthesia (n = 6 mice, 3 urethane anesthetized, 3 ketamine anesthetized). Anesthesia causes a rightward shift (i.e., broader tuning) in the anesthetized state.

(D) Cumulative frequency plot of the peak response amplitude for all mitral cell-odor pairs that were responsive in both the awake and anesthetized state (567 pairs). Anesthesia causes a rightward shift (i.e., larger responses) in the anesthetized state.

(E) The fraction of trials with correct odor classification plotted against the number of responsive cell-odor pairs used for the classification. In the awake state, fewer responsive cell-odor pairs are required for high levels of correct classification. Dotted line represents the chance level of classification.

(F) Mitral cell responses are more temporally dynamic in the awake state. Top: heat maps of the activity of all responsive mitral cell-odor pairs in awake and anesthetized states (awake: 824 cell-odor pairs; anesthetized: 1,218 cell-odor pairs), sorted by their onset times. Bottom: histograms of the onset times of all responsive cell-odor pairs in the two states show that responses are temporally more diverse in the awake state, while responses under anesthesia are more time locked to odor onset. Dashed lines indicate the odor period.

RESULTS

Chronic Imaging of Mitral Cell Activity with GCaMP3

We expressed GCaMP3 (Tian et al., 2009) specifically in olfactory bulb principal cells (mitral and tufted cells) by injecting a Cre recombinase-dependent viral vector (Atasoy et al., 2008) into the olfactory bulbs of protocadherin-21 (PCdh21)-Cre mice, which express Cre exclusively in olfactory bulb principal cells (Nagai et al., 2005). Several weeks after injection, virtually all glomeruli had GCaMP3-expressing dendrites, and immunostaining with a mitral/tufted cell-specific antibody (Tbx21) (Yoshihara et al., 2005) showed that the majority of Tbx21-positive cells (67%, n = 3 mice, 644 cells) express GCaMP3 (Figure 1B). Consistent with the selective expression in mitral/tufted cells, all GCaMP3-expressing cells (n = 2 mice, 323 cells) lacked immunoreactivity for GAD67, a marker for GABAergic interneurons (data not shown). We next performed simultaneous patch-clamp recording and two-photon imaging in olfactory bulb slices to test the ability of GCaMP3 to report action potential firing in mitral cells (GCaMP3-expressing cells in the mitral cell layer). We measured GCaMP3 fluorescence changes in mitral cells in response to spikes elicited at 50–100 Hz via brief depolarizing current steps (1 nA, 3 ms). In agreement with previous findings in cortical pyramidal cells (Tian et al., 2009), we found that increases in GCaMP3 fluorescence had a relatively linear relationship with the number of action potentials evoked in mitral cells (Figures 1C and 1D).

To optically monitor mitral cell activity in vivo, we implanted a cranial window (Holtmaat et al., 2009) over the dorsal olfactory bulb of GCaMP3-expressing mice. Using two-photon imaging selectively in the mitral cell layer allowed us to repeatedly image the same sets of up to 100 mitral cells over months in awake, head-fixed mice (Dombeck et al., 2007; Komiyama et al., 2010) (Figures 1E and 1F). Consistent with previous electrophysiological studies in anesthetized animals (Bathellier et al., 2008; Davison and Katz, 2007; Dhawale et al., 2010; Fantana et al., 2008; Meredith, 1986; Mori et al., 1992; Tan et al., 2010), passive application of structurally diverse odors elicited activity revealed by increases in GCaMP3 fluorescence in overlapping but distinct ensembles of mitral cells (Figure 1G).

Wakefulness Sparsens Mitral Cell Odor Responses

To study how odor representations in awake animals differ from those under anesthesia, we imaged responses of the same mitral cell populations to a set of seven structurally diverse odors before and after inducing anesthesia. The transition from the awake to anesthetized brain state (monitored by the loss of fast-wave EEG activity) greatly enhanced odor-evoked ensemble activity: odors elicited stronger mitral cell responses and the density of odor representations increased (Figures 2A and 2B). Under anesthesia, individual mitral cells respond to more odors (Figure 2C) and responses are stronger (Figure 2D). This increase in mitral cell responsiveness during anesthesia is not due to an increase in sensory input to the bulb (see Figure S1 available online). The effects of anesthesia were indistinguishable with ketamine and urethane, two commonly used and chemically distinct anesthetics (Figure S2), suggesting that the differences in mitral cell activity reflect changes in brain state rather than local pharmacological effects of the drugs. Mitral cell spontaneous firing rates are reportedly higher in the awake versus anesthetized state (Adrian, 1950; Rinberg et al., 2006a). To test whether changes in baseline activity between awake and anesthetized states could account for the differences in the normalized measure of mitral cell responses (dF/F), we next compared the odor-induced fluorescence changes without normalization between the two states. The enhancement of mitral cell responses with anesthesia was apparent even in this unnormalized measure (Figure S2), indicating that anesthesia increases the absolute amplitudes of mitral cell odor responses.

We next examined how differences in mitral cell ensemble responses in awake and anesthetized states affect odor coding by determining the efficiency of cell ensembles to discriminate between the seven odors. To quantify the efficiency of odor coding, we calculated the fraction of odor trials that are classified correctly using responses for the entire duration of odor stimulation when we randomly sampled different numbers of responsive mitral cell-odor pairs (see Experimental Procedures). In the awake state, fewer mitral cell responses were needed to achieve high levels of correct classification compared to the anesthetized state (Figure 2E). These results indicate that compared to the anesthetized brain state, the selective odor tuning of mitral cells and sparse odor respresentations during wakefulness are more efficient at odor coding.

In addition to the effects of anesthesia on mitral cell odor tuning, there was a marked difference in the temporal dynamics of mitral cell responses between awake and anesthetized brain states. When mice are awake, odor responses are temporally diverse, with the onset timing of different cell-odor pairs fairly evenly tiling the period of odor stimulation and a few seconds after odor offset (Figure 2F, left). However, in the anesthetized state, mitral cell responses are less dynamic, such that the majority of responsive cells exhibit onset times near the

(G) Average (solid) and SEM (shading) of correlation coefficients of ensemble activity patterns and the initial patterns (average of 0.75–1.25 s after odor onset) as a function of time in all mouse-odor pairs (42 pairs: six mice, seven odors). Awake responses become progressively more decorrelated from the initial patterns over time than responses under anesthesia.

(H) Principal component analysis (PCA) reveals that odor representations become more distinct over time in the awake state compared to anesthetized brain states. The ensemble activity patterns of mitral cells pooled across animals (n = 6 mice) from 49 trials (seven trials/seven odors, 4 s odor application) each in the awake and anesthetized states are plotted in the space of the first three principle components defined by concatenating responses in both states (Experimental Procedures). Plots show ensemble activity under baseline conditions (preodor), early during odor application (0–1 s), and during the last second of odor application (3–4 s). Activity patterns elicited by different odors are more distinct in the awake state, especially during the later phase of odor stimulation. Points represent individual trials. Green, isoamyl acetate; red, ethyl butyrate; black, heptan-4-one; light blue, heptanal; yellow, butyric acid; purple, cyclohexanone; blue, ethyl tiglate.

(I) The ability of cell ensembles to correctly classify odors improves over time during odor presentation. The temporal improvement is greater in the awake state. Odor onset = 0 s. See also Figures S1 and S2.

beginning of the odor stimulus (Figure 2F, right). Analysis of the correlation coefficients of ensemble responses at different time points with the initial activity patterns (time average of 0.75–1.25 s after odor onset) confirmed that ensemble activity patterns became more decorrelated over time in the awake versus anesthetized state (Figure 2G). We performed principal component analysis to explore how the different temporal dynamics of odor responses in the awake and anesthetized state contributed to the ability of mitral cell ensembles to distinguish different odors over time. Representations of odor-evoked activity as a function of time in principal component space revealed that ensemble activity patterns for different odors were more separated in the awake state, and the separation in the awake state significantly improved over time (Figure 2H). This temporal improvement of odor classification in the awake state was confirmed when we considered the fractions of correctly classified trials, using responses in increasing time windows. Considering the numbers of responses that gave the same levels of correct classification in awake and anesthetized states during the first second of odor stimulus (awake: 15 responses; anesthetized: 25), we find that odor classification improved over the course of odor stimulation more strongly in the awake state (Figure 2I). Thus, the improvement of classification efficiency in the awake state is partly due to the odor-specific temporal dynamics. Taken together, these results indicate that odor representations in the awake state are more sparse, temporally dynamic, and efficient, compared to anesthetized brain states.

Wakefulness Enhances Granule Cell Activity

Granule cells are a major class of GABAergic interneurons in the olfactory bulb that mediate mitral cell recurrent and lateral inhibition via dendrodendritic synapses (Isaacson and Strowbridge, 1998; Schoppa et al., 1998; Yokoi et al., 1995). Therefore, we next considered the possibility that differences in mitral cell odor representations between awake and anesthetized states could reflect differences in granule cell activity. We expressed GCaMP3 by injecting a nonconditional viral vector in the olfactory bulb granule cell layer of wild-type mice. Several weeks after injection, dense sets of neurons in the granule cell layer were visible through a cranial window (Figure 3A). While the vast majority of neurons in this layer are granule cells, our sample probably contains a small fraction of short axon cells, a heterogeneous class of interneurons in the granule cell layer (Eyre et al., 2008; Pressler and Strowbridge, 2006).

In awake mice, a large fraction of granule cells showed spontaneous increases in GCaMP fluorescence that are sometimes temporally correlated to one another (Figure 3B, top). Similar to mitral cells, odors activated ensembles of granule cells in awake mice (Figures 3C and 3D). The odor tuning in the awake state was similar between granule cells (Figure 3E) and mitral cells (Figure 2C). Remarkably, after the induction of anesthesia, the spontaneous activity of granule cells virtually disappeared (Figure 3B, bottom). Furthermore, in contrast to mitral cells, anesthesia strongly reduced odor responses of granule cells (Figures 3C and 3D). This resulted in individual granule cells responding to fewer odors with weaker responses under anesthesia (Figures 3E and 3F). Both ketamine and urethane caused similar decreases of odor-evoked activity in granule cells (Figure S2). In the awake state, many granule cells responded near the onset of odor stimulation (Figure 3G, left) and the temporal dynamics of granule cell responses did not appear to be strongly modulated by brain states (Figure 3G). Thus, both spontaneous and odor-evoked activity of granule cells are much weaker in the anesthetized state, indicating that the activity of local inhibitory circuits in the olfactory bulb is strongly enhanced during wakefulness.

Daily Odor Experience Leads to a Gradual, Odor-Specific Reduction in Mitral Cell Activity

Having identified major differences in olfactory bulb circuits in the awake and anesthetized state, we next asked how odor experience shapes mitral cell odor representations in awake animals. We imaged mitral cell responses to a panel of seven structurally diverse odors applied on 2 successive days (eight trials of each odor/day, 4 s/trial for this and all subsequent experiments). Because we used naive mice that had never been tested with odors, we considered all tested odors as "novel." On the first day of testing, each odor activated a large subset of the simultaneously imaged mitral cell population. However, responses of the same mitral cell population to the same odors 1 day later were significantly different (Figure 4A). Examining the response of each mitral cell to each odor, we found that while only 4% of odor-cell pairs showed a significant increase in response magnitude, 27% showed a significant decrease ($n = 3$ mice, 151 mitral cells, $p < 0.01$, permutation test, 10,000 repetitions for this and all following analyses unless otherwise mentioned). Consequently, the same odors activated significantly lower proportions of mitral cells on day 2 compared to day 1 (day 1: 27.3% ± 3.2% versus day 2: 21.1% ± 2.5%, mean ± SEM; $p < 0.01$, paired permutation test, 10,000 repetitions). Thus, the population responses to each odor became weaker after only 1 day of brief odor experience, indicating that odor experience has a lasting effect on the way mitral cells represent olfactory information.

We next considered whether the weakening of odor representations induced by odor experience reflects a nonspecific decrease in mitral cell responsiveness or is specific to the experienced odors. To address this, we assessed the difference between responses to two sets of odors (A and B, randomly chosen for each mouse), where set A odors were experienced daily for 7 days, while set B odors were only encountered on the first and last days (Figure 4B, $n = 5$ mice, 212 mitral cells). Strikingly, mitral cell responses to set A odors progressively declined over days, while there was little change in the responses to set B odors on day 7 (Figure 4C and Figure S3). To quantify the changes in mitral cell responses, we calculated the change index (CI) for each responsive mitral cell-odor pair on each trial (trial X) of a given day as (response on trial X – the initial response on day 1)/(response on trial X + the initial response on day 1). Thus, CI ranges from −1 to 1, where a value of −1 represents a complete loss of response, 1 represents emergence of a new response, and 0 represents no change. On the first day of testing (day 1), the average CI values for both odor sets A and B steadily declined during repeated odor exposure (Figure 4D). During days 2–6, the CI value for set A odors progressively decreased with little recovery from previous days and reached a steady-state value after 4–5 days of daily

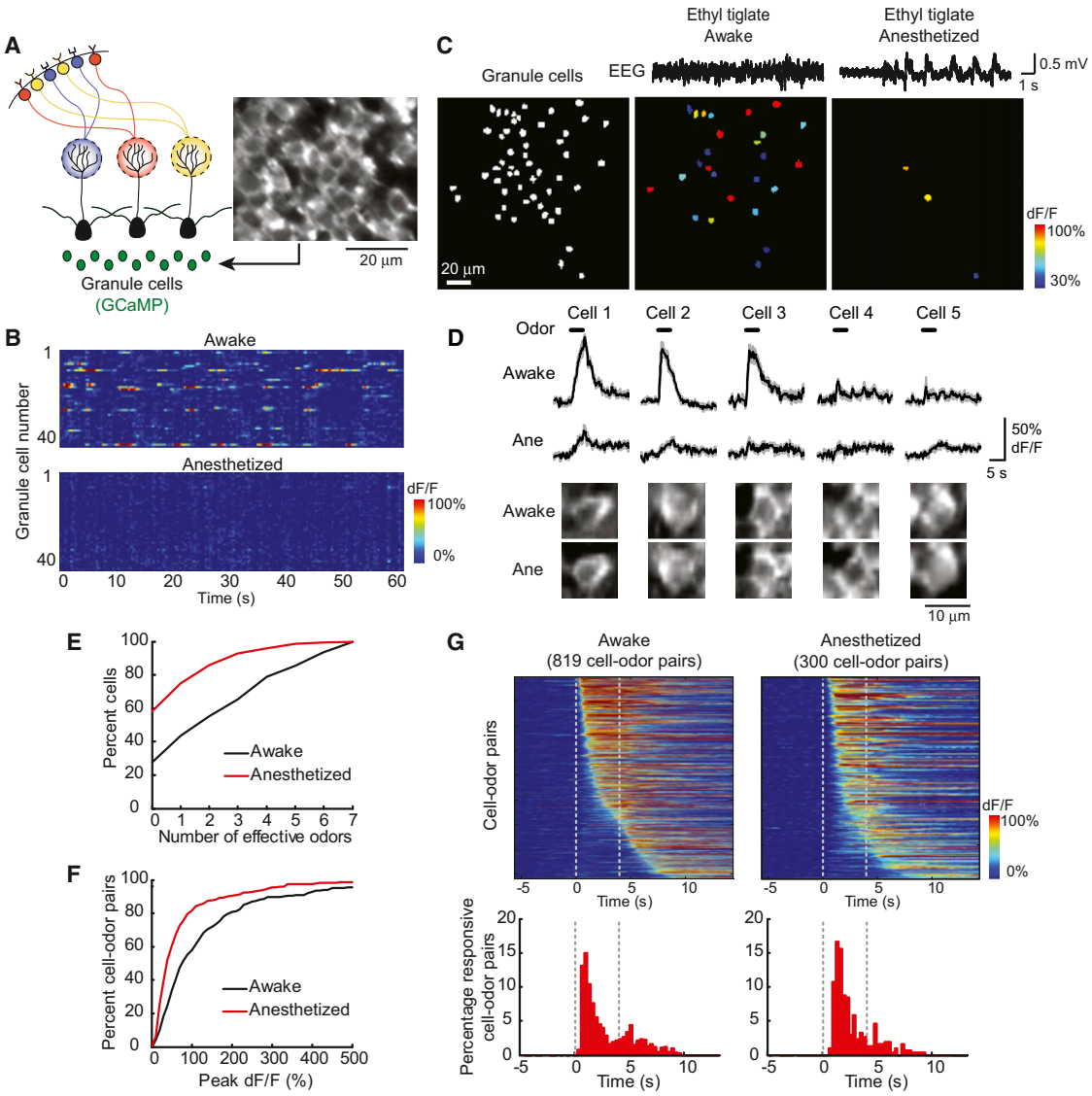

Figure 3. Granule Cell Activity Is Enhanced during Wakefulness

(A) Left: schematic of granule cell imaging. Right: a field of granule cells imaged in vivo.

(B) Spontaneous activity of a population of granule cells (n = 43) imaged in the awake and anesthetized states over 60 s in each condition. In the awake state, many granule cells show spontaneous increases in GCaMP fluorescence, which is virtually absent in the anesthetized state.

(C) Granule cell odor-evoked activity maps (pseudocoloring represents odor-evoked GCaMP3 dF/F response averaged across seven trials) from a mouse recorded in both the awake and anesthetized state. Granule cell ensembles respond more strongly to the same odor in the awake state (middle) compared to under anesthesia (right). The left panel shows all imaged granule cells in white. Top traces are example EEG traces in both states.

(D) Average (solid lines) and SEM (shading) of odor-evoked GCaMP3 responses from five granule cells in (C) during awake and anesthesized states show a decrease in odor-evoked activity after the induction of anesthesia. Images at the bottom show that each granule cell was clearly identified under both conditions.

(E) Summary data shown in cumulative frequency plot of odor tuning (the number of odors eliciting responses out of the seven tested odors) for 336 granule cells in the awake state compared to after induction of anesthesia (n = 6 mice, 3 urethane anesthetized, 3 ketamine anesthetized). Anesthesia causes a leftward shift (i.e., narrower tuning).

(F) Cumulative frequency plot of the peak response amplitude of all granule cell-odor pairs that were responsive in both the awake and anesthetized state (222 pairs) shows a leftward shift (i.e., smaller responses) in the anesthetized state.

(G) Temporal dynamics of granule cell odor responses. Top: heat maps of the activity of all responsive granule cell-odor pairs in awake and anesthetized states (awake: 819 cell-odor pairs; anesthetized: 300 cell-odor pairs), sorted by their onset times. Bottom: histograms of the onset times of all responsive cell-odor pairs in the two states. Dashed lines indicate the odor period. See also Figure S2.

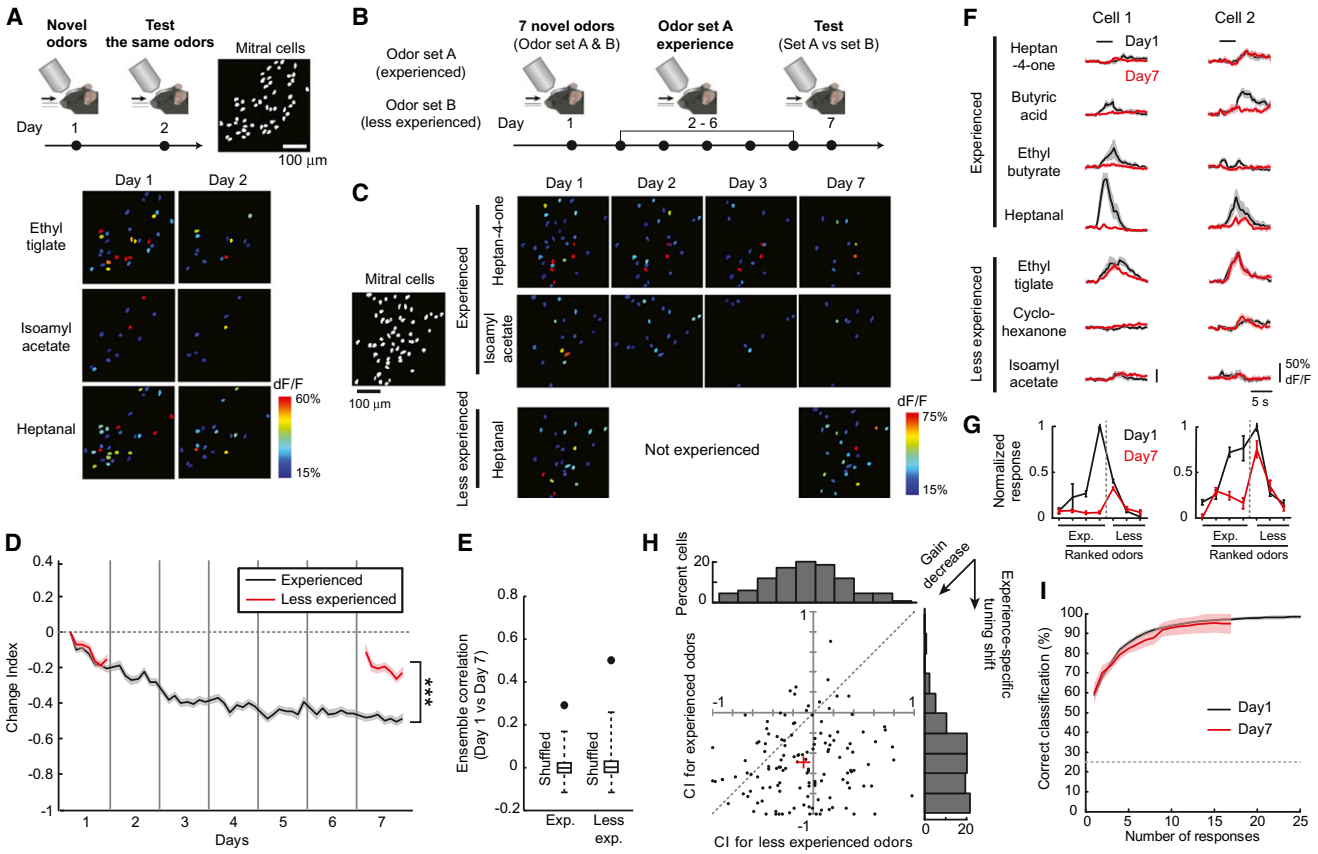

Figure 4. Odor Experience Leads to a Gradual and Odor-Specific Reduction of Mitral Cell Responses

(A) Mitral cell odor-evoked activity maps (pseudocoloring represents odor-evoked GCaMP3 dF/F response averaged across seven trials) from a mouse imaged on 2 consecutive days. Mitral cell ensembles respond more weakly to the same series of novel odors on the second day of testing. The top right panel shows all imaged mitral cells in white.

(B) Odor experience and chronic imaging protocol.

(C) Activity maps of mitral cell population responses from one mouse show that responses to experienced (odor set A) odors become weaker after 7 days (day 7), while responses to less-experienced (odor set B) odors remain relatively stable.

(D) Average (solid) and SEM (shading) of change index (CI, see text) for each trial across days. On day 7, responses to experienced odors are significantly weaker than those to less-experienced odors. ***$p < 0.001$.

(E) Correlations of odor representations across days for each odor set, measured by Pearson's correlation between population vectors that were constructed by concatenating responses of each odor-cell pair. For both odor sets, the measurements (black dots) were higher than shuffled data (10,000 repetitions in which ROI labels were shuffled within each odor-animal pair), which are shown in box plots in which whiskers represent most extreme values within 1.5× interquartile range. These data indicate that ensemble response patterns are conserved after odor experience.

(F) Individual mitral cells show odor-specific plasticity, such that responses to experienced odors are generally reduced, while responses to less-experienced odors are largely unaffected. Average (solid lines) and SEM (shading) of odor-evoked GCaMP3 responses from two mitral cells in the same mouse on the first day of testing (day 1, black) and after 7 days of experience with a subset of odors (day 7, red).

(G) Tuning curves of the two cells in (F) (odors ranked for each cell according to the response strength on day 1) indicate a shift in tuning toward less-experienced odors on day 7.

(H) Summary of odor-specific response plasticity of individual mitral cells that responded to both odor sets A and B (n = 134). Each black point represents an individual mitral cell, whose y and x positions show the average CI values for experienced and less-experienced odors, respectively. Red cross represents average of all cells. If the cells show the same amount of plasticity for experienced and less-experienced odors (i.e., a simple gain change), they would fall along the dashed unity line. The distribution shows a clear separation away from the unity line ($p < 0.001$, bootstrap, 10,000 repetitions) with CI values <0 for experienced odors and CI values ≈0 for less-experienced odors, indicating that a specific tuning shift occurs in a large number of mitral cells. Histograms indicate the distribution of CI values for the experienced (right) and less-experienced (top) odor groups for each cell.

(I) The fraction of trials classified correctly for four experienced odors (odor set A) on day 1 and day 7 plotted against the number of responsive cell-odor pairs used for the classification. Odor coding efficiency by mitral cell ensembles is unchanged after 7 days of odor experience. n = 5 mice. Dotted line represents the chance level of classification. See also Figures S3–S7.

experience. When responses to both odor sets were tested on day 7, the average CI value for the less-experienced odors (set B) was significantly greater than that of the experienced odor set (Figure 4D, $p < 0.001$). Mitral cell-odor pairs whose response onset times are during odor stimulation ("on" responses) and after odor stimulation ("off" responses)

showed similar experience-dependent plasticity on day 7, with a trend for "on" responses to be more strongly affected (CIs for the experienced odor set are the following: "on" response: −0.585 ± 0.016; "off" response: −0.383 ± 0.019. CIs for the less-experienced odor set are the following: "on" response: −0.272 ± 0.022; "off" response: −0.158 ± 0.023). Changes in raw dF/F values or fractions of responsive cells also support odor specificity of the plasticity (Figure S4). We did not detect significant changes in respiration rates throughout the course of the experiment (respiration rates during all odor trials were the following: on day 1: 3.39 ± 0.20 Hz versus on day 7: 3.44 ± 0.19 Hz, $p = 0.900$; on day 7, experienced odor trials: 3.36 ± 0.21 Hz versus less-experienced odor trials: 3.47 ± 0.19 Hz, $p = 0.757$). In addition, CI did not correlate with differences in the levels of GCaMP3 expression across cells (Figure S4). The slight deviation from zero in CI for set B odors at the beginning of testing on day 7 is not related to the number of set A odors each cell responds to (Figure S4) and is similar to what was observed in a separate set of animals, which only experienced odors on day 1 and day 7 (Figure S5). This suggests that the small change in CI for set B odors on day 7 is not due to nonspecific effects of set A odors, but rather reflects the fact that experience with set B odors on day 1 causes a weak but long-lasting reduction in responsiveness. Together, these results indicate that the weakening of mitral cell odor representations occurs within each day, accumulates over days of experience, and is specific to experienced odors. After this experience-dependent plasticity, odor representations still resembled their original patterns, shown by the highly significant correlations between ensemble responses on day 1 and day 7 for both odor sets (Figure 4E). Furthermore, similar odor-specific modulation of mitral cell activity was observed when mice experienced odors in their home cage, or when mice were tested with odors with a lower concentration, indicating that the plasticity is independent of our imaging conditions (Figures S5 and S6).

The odor-specific reduction in the responses of mitral cell populations could reflect two different mechanisms. First, the mitral cells that preferentially respond to experienced odors might become less responsive to all odors (gain decrease), in which case experience would not lead to a change in their odor tuning properties. Alternatively, experience could selectively reduce the mitral cell responses to the experienced odor set, which would modify the odor tuning of individual cells. To distinguish between these two possibilities, we examined the tuning properties of mitral cells that responded to both the experienced and less-experienced odor sets. Remarkably, we observed that individual mitral cells show experience-dependent changes in odor tuning. After odor set A experience, many cells showed decreased responsiveness specifically to set A odors, while maintaining responsiveness to set B odors (Figure 4F). This was apparent as a specific modulation of the odor tuning curves of individual cells (obtained from the seven tested odors in which odors from the two sets are rank ordered based on responses of individual cells). After experience, odors that generated the strongest responses were shifted toward those that were less experienced (Figure 4G). This specific shift in tuning was consistently observed when CI values were determined for the experienced and less-experienced odor sets for all individual cells (Figure 4H). In terms of ensemble coding, odor classification by mitral cell ensembles was equally efficient before and after experience-dependent plasticity (Figure 4I).

What effect does experience have on granule cells? To address this question, we imaged granule cell activity in a separate set of animals during the same 7 day odor experience protocol. Similar to mitral cells, we found that responses of individual granule cells also decreased specifically to experienced odors (Figure S7), even though the effect of experience was smaller in granule cells compared to mitral cells (the reduction in the fraction of responsive cells was 70.0% ± 4.3% for mitral cells versus 38.4% ± 6.5% for granule cells, $p < 0.001$). The reduction in granule cell activity is not unexpected given the fact that mitral cells are the major source of excitation onto this class of interneurons and suggests that the experience-dependent plasticity of mitral cell responses is unlikely to reflect a global increase in the activity of granule cells.

Odor Experience-Dependent Plasticity Is Not Due to Changes in OSN Input

We next asked whether experience-dependent changes in odor representations could be explained by plasticity at the level of sensory inputs to the bulb. To test this idea, we performed chronic imaging of the activity of olfactory sensory neuron synapses in the glomerular layer using OMP-synapto-pHluorin mice (Bozza et al., 2004), in which all OSNs express synapto-pHluorin, a reporter of neurotransmitter release (Figure 5A). We imaged OSN transmission with the same 1 week protocol used for studying mitral cell plasticity (Figure 5B). Each odor activated a unique ensemble of glomeruli (Figure 5C), consistent with previous reports (Belluscio and Katz, 2001; Bozza et al., 2004; Igarashi and Mori, 2005; Johnson et al., 2005; Onoda, 1992; Rubin and Katz, 1999; Stewart et al., 1979; Wachowiak and Cohen, 2001; Xu et al., 2000, 2003; Yang et al., 1998). In stark contrast to mitral cell activity, presynaptic input to the bulb remained stable over the course of the experiment for both experienced and less-experienced odors (Figures 5C–5E). This is not due to saturation of the synapto-pHluorin signal, since higher odor concentrations triggered stronger responses (Figure S1). In addition, mitral cell glomerular GCaMP3 responses, which reflect a combination of local synaptic excitation of mitral cell dendrites by OSN input and backpropagating action potentials, show only a modest reduction during the same odor experience protocol (Figure S8). Thus, these results indicate that experience-dependent plasticity of mitral cell activity must be generated by changes downstream of sensory neuron input to the bulb.

Odor Experience-Dependent Plasticity Gradually Recovers over Months and Is Repeatable

Does the response plasticity of mitral cells to experienced odors happen only once in the lifetime of an animal and leave a permanent "imprint" of odor experience or is this a dynamic process that shapes odor representations throughout life? To

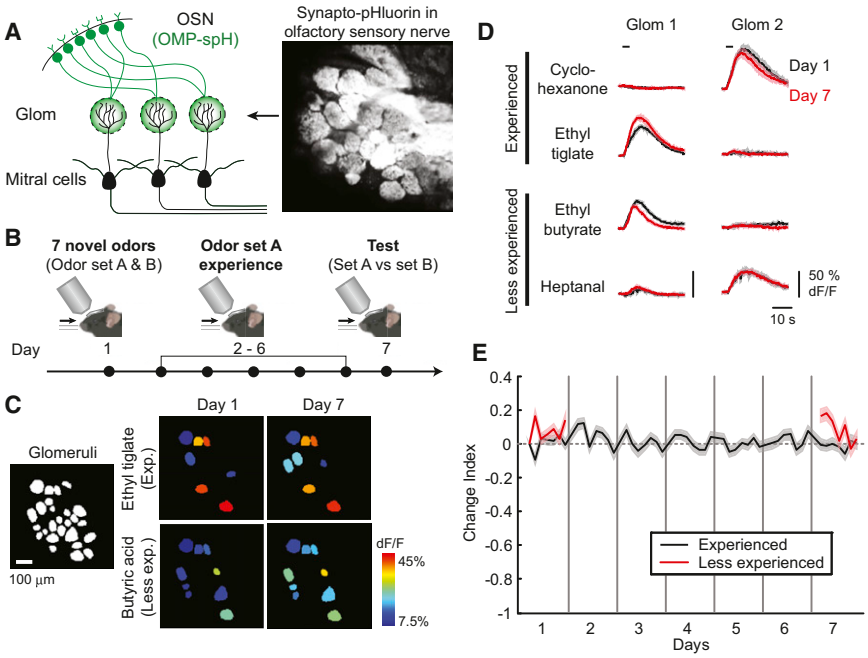

Figure 5. Sensory Neuron Input to the Olfactory Bulb Is Unaltered by Repeated Odor Experience

(A) Schematic illustrating expression of optical reporter of transmitter release in OSNs.

(B) Odor experience and chronic imaging protocol.

(C) Odor-evoked glomerular activity maps from an OMP-spH mouse reveal that OSN transmission is unaltered by odor experience.

(D) Average (solid lines) and SEM (shading) of odor-evoked synapto-pHluorin responses from two glomeruli in the same mouse on the first day of testing (day 1, black) and after 7 days of experience with a subset of odors (day 7, red).

(E) Summary data (n = 79 glomeruli from 4 mice) indicating that synapto-pHluorin responses remain stable (change index near 0) throughout the course of the experiment. See also Figures S1 and S8.

distinguish these possibilities, we examined the persistence of the effect of odor experience by testing odor responses at various time points after home cage rearing without additional odor applications (Figure 6A, "recovery"). Seven days of home cage rearing led to a partial recovery of mitral cell responses. Further recovery was seen after 3 more weeks, and responses recovered completely after 2 months (Figures 6B and 6C). Odor representations after full recovery resembled those on the initial day (day A1, Figure 6D). Thus, the effect of odor experience on mitral cell responses persists for weeks but not months.

After full recovery of the plasticity to odor set A, we repeated the 1 week odor experience protocol, this time using odor set B for the experienced odors (Figure 6A, "odor set B experience," n = 3 mice, 132 mitral cells). After 1 week of daily experience with odor set B, the responses of mitral cells were selectively reduced to set B odors while their responses to set A odors were maintained (Figures 6B and 6C). Furthermore, the magnitude and time course of the modulation of the population response were virtually identical for the two separate bouts of odor experience (Figure 6C). We determined how mitral cell tuning was modulated over time in this experiment by measuring the relative odor preference of individual cells to the two odor sets ([odor set A response – odor set B response] / [odor set A response + odor set B response]). Mitral cell tuning consistently shifted toward a preference for the less-experienced odors (Figure 6E). This experience-dependent shift in odor preference is also apparent from averaging the tuning curves of all individual cells (Figure 6F); the initial experience (odor set A) caused less-experienced odors (set B) to become more preferred stimuli and after recovery, experience of odor set B led to a shift in the opposite direction. Since the total odor exposure was the same for both odor sets on the final day of testing (day B7), we could determine the net effect of recent versus remote experience on the population response. Comparing the fraction of mitral cells activated by the two odor sets revealed that recently experienced odors are much more sparsely represented than those that were frequently experienced months before testing (Figure 6G).

The Expression of Experience-Dependent Plasticity of Mitral Cell Responses Depends on Wakefulness

Our results indicate that brief odor experience weakens subsequent mitral cell responses in an odor-specific manner. However, previous studies have reported stable mitral cell responses to brief odor experience, while prolonged odor exposure (30 s to minutes) leads to a decrease in responsiveness that is relatively odor nonspecific (Chaudhury et al., 2010; Wilson, 2000; Wilson and Linster, 2008). A key difference is that these previous studies recorded mitral cell activity under anesthesia, while our current study reports mitral cell activity in awake animals.

To test whether wakefulness governs the experience-dependent plasticity of mitral cell responses, we imaged mitral cell responses to brief, repeated odor exposure in naive mice anesthetized with urethane (n = 5 mice, 171 mitral cells) or ketamine (n = 2 mice, 150 mitral cells). We found that odor-evoked mitral cell responses are stable under anesthesia during repeated exposure to novel odors, in stark contrast to the results from awake mice that experienced the same novel odors for the same number of trials (Figure 7A). We next asked whether anesthesia modifies the expression of experience-dependent plasticity once it has been induced in awake mice. To address this question, we tested the effect of daily repeated odor experience in another set of awake mice (n = 4 mice, 221 mitral cells) and additionally imaged responses of the same mitral cells to the same odors during ketamine anesthesia on day 1 and day 7 (Figure 7B). As expected, anesthesia increased odor-evoked mitral cell responses on day 1. As in previous experiments (Figure 4), the CI value for experienced odors progressively decreased during days 2–6 and the odor-specific weakening

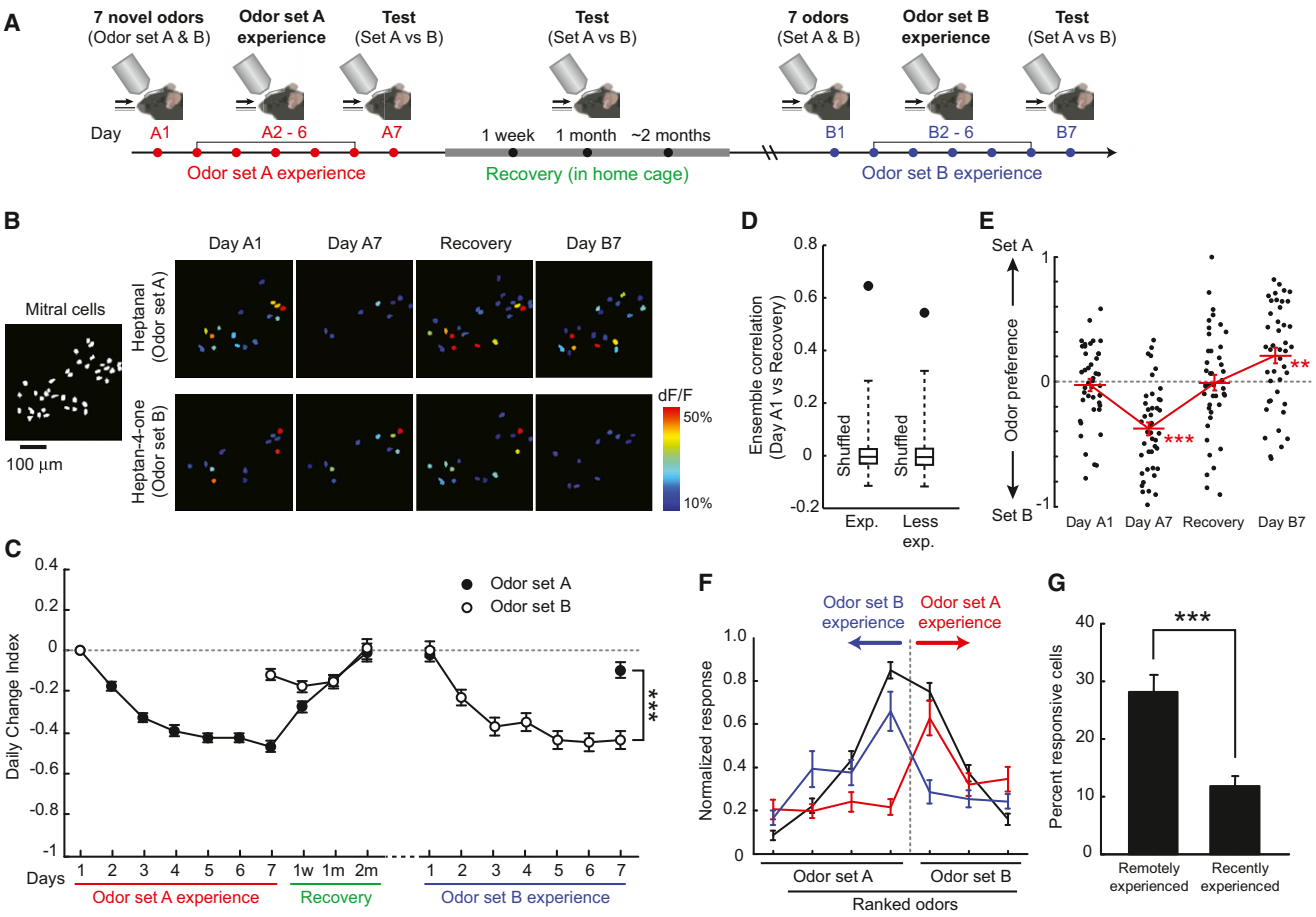

Figure 6. Dynamic Modulation of Sensory Representations and Mitral Cell Tuning by Recent Experience

(A) Schematic of the months-long experimental protocol, in which responses of the same mitral cell populations were imaged during odor set A experience, recovery, and subsequent odor set B experience.

(B) Mitral cell activity maps from a representative mouse over the course of the experiment. Imaging time points correspond to days illustrated in (A). Recovery, 2 months. Recently experienced odors (set A on day A7 and set B on day B7) are more weakly represented than novel odors (sets A and B on day 1) or odors with distant experience (set B on day A7 and set A on day B7).

(C) Summary of CI values, defined for responses on each day, over the time course of the experiment (n = 132 mitral cells from 3 mice).

(D) After recovery, odor representations are similar to those measured on day A1. See legend for Figure 4E.

(E and F) Tuning of individual mitral cells is dynamically modulated by recent experience.

(E) Odor preference for individual cells (n = 43, black points) for set A or set B odors shifts with experience. Only cells that responded to at least one odor from each odor set on day A1 and at least one odor from either set at the other times are included. Red marks indicate average and SEM.

(F) Tuning curves for odors in each set ranked based on the response strength on day A1 (black). Odor set A experience initially shifts the tuning curve toward odor set B. After recovery, odor set B experience shifts the tuning curve toward odor set A.

(G) Average fraction of responsive mitral cells to odor set B on day B7 (recently experienced) is significantly less ($p < 0.001$, bootstrap, 10,000 repetitions) than the fraction of cells responsive to odor set A (remotely experienced). n = 12 and 9 mouse-odor pairs for remote and recent, respectively. $^{**}p < 0.01$, $^{***}p < 0.001$.

of mitral cell responses was observed on day 7. Immediately after these awake trials on day 7, mice were again anesthetized and the responses of the same mitral cell populations to the same two odor sets were imaged. Remarkably, mitral cell responses under anesthesia on day 7 were indistinguishable from those observed during anesthesia on day 1; thus, the expression of the plasticity induced during wakefulness was blocked when tested under anesthesia (Figure 7B). These results indicate that the expression of the experience-dependent plasticity of mitral cell responses depends critically on wakefulness.

DISCUSSION

Odor Coding in Awake and Anesthetized Brain States

Although previous studies reported that odor-evoked mitral cell activity is enhanced under anesthesia (Adrian, 1950; Rinberg et al., 2006b), how odor coding by mitral cell ensembles differs in the awake and anesthetized state is unclear. In this study, we show that the transition from the awake to anesthetized brain state has a dramatic impact on how olfactory information is represented by ensembles of mitral cells. By imaging large populations of mitral cells in individual mice, we find that odor-evoked

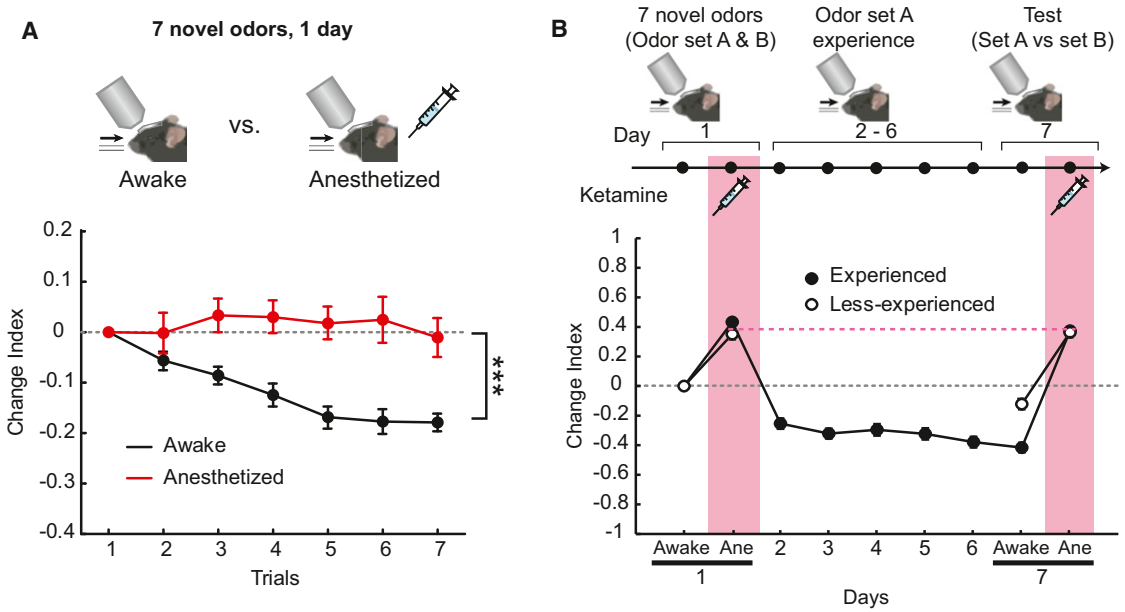

Figure 7. The Expression of the Experience-Dependent Plasticity of Mitral Cell Activity Depends on Wakefulness

(A) Change index for each trial within a day in awake (black) and anesthetized (red) animals. Responses under anesthesia are significantly more stable compared to those in awake animals, which show significant weakening. Error bars represent SEM. ***$p < 0.001$.

(B) Activity of mitral cell populations imaged over a 7 day experience protocol. Additionally, activity of the same mitral cell populations to the same odors was imaged under ketamine/xylazine anesthesia on days 1 and 7. Summary of change index values, defined for responses on each day, over the time course of the experiment shows that the odor-specific reduction in mitral cell activity observed during wakefulness on day 7 was abolished when subsequently tested under anesthesia. Error bars (SEM) are contained in symbols.

ensemble activity is much sparser and more temporally dynamic in the awake state and that anesthesia increases the density of odor representations by broadening the odor tuning of mitral cells. Importantly, we also show that the sparse and temporally dynamic ensemble activity during wakefullness is more efficient for odor population coding: compared to anesthetized brain states, fewer mitral cell responses in the awake state are required for accurate odor discrimination.

The temporal dynamics of mitral cell ensemble activity have been proposed to contribute to odor coding (Bathellier et al., 2008; Friedrich et al., 2004; Friedrich and Laurent, 2001; Laurent et al., 1996; Mazor and Laurent, 2005). Indeed, here we demonstrate that odor classification in the awake state improves gradually as odor representations develop over time. In contrast, the temporal dynamics of odor representations are reduced in the anesthetized brain state, which contributes to a reduction in the population coding efficiency. We note that the temporal resolution of our imaging approach (~6.3 Hz) precludes the assessment of finer temporal features of mitral cell responses (Bathellier et al., 2008; Cury and Uchida, 2010; Shusterman et al., 2011). Nevertheless, our results reveal a strong temporal component to mitral cell odor representations in awake animals, which may be underestimated in recordings under anesthesia. Variability in respiratory behavior in the awake state could contribute to the temporal dynamics of mitral cell responses (Carey and Wachowiak, 2011; Verhagen et al., 2007). However, as we discuss below, the opposite effects of anesthesia on mitral cells and granule cells make it unlikely that respiration variability can fully account for the changes and we suggest that actions of local inhibitory circuits probably play an important role.

Enhanced Activity of Inhibitory Granule Cells during Wakefulness

Anatomical and electrophysiological studies have suggested that granule cells are the major class of GABAergic interneurons in the olfactory bulb that shape mitral cell response properties through recurrent and lateral inhibition via dendrodendritic synapses (Isaacson and Strowbridge, 1998; Schoppa et al., 1998; Shepherd et al., 2004; Yokoi et al., 1995). However, the direct measurement of granule cell activity in vivo has been limited to a few studies performed in anesthetized animals (Cang and Isaacson, 2003; Tan et al., 2010), hampering our understanding of the operation of olfactory bulb inhibitory interneurons in the awake state. Attempts to estimate the effect of anesthesia on granule cell activity with extracellular recording of field potentials (Nicoll, 1972; Stewart and Scott, 1976; Tsuno et al., 2008) have reached inconsistent conclusions, reflecting the difficulty of interpreting these indirect measurements.

Here we report, to our knowledge, the first direct in vivo measurements of granule cell activity in awake animals. Granule cells respond to odors rapidly, and their tuning properties are similar to those of mitral cells. Strikingly, anesthesia caused a substantial attenuation of both spontaneous and odor-evoked granule cell activity, which is in stark contrast to the enhancement of odor-evoked activity of mitral cells in the anesthetized state. The reduction of granule cell activity in the anesthetized

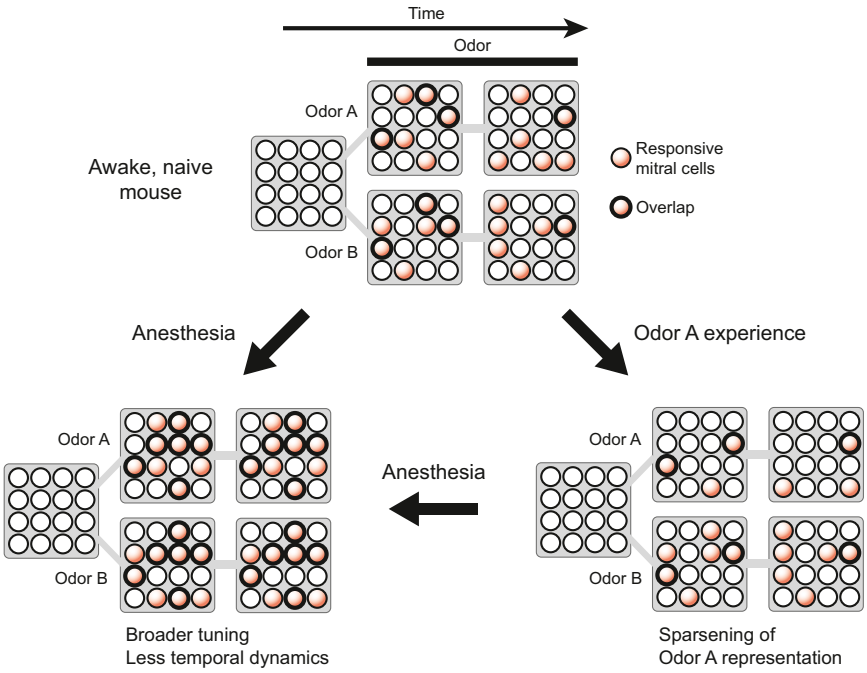

Figure 8. Schematic of Dynamic Odor Representations

In the awake state, odors are represented by sparse and temporally dynamic patterns of mitral cell ensemble activity. Odor experience leads to a further sparsening of representations of experienced odors. Anesthesia broadens mitral cell responses and reduces temporal dynamics, resulting in a greater overlap of representations of different odors and a reduced efficiency of odor coding.

state is consistent with previous intracellular recordings under anesthesia, which reported a low probability of odor-evoked action potentials in granule cells (Cang and Isaacson, 2003) and indicates that granule cell recordings under anesthesia have underestimated their actions in the awake state. We think it is unlikely that the anesthetics are directly changing the intrinsic excitability of granule cells, since the two chemically distinct anesthetics (ketamine and urethane) had the same effect on granule cell activity. Rather, the effect of the anesthetics is likely to reflect modulation of brain state. For example, granule cells are a major target of centrifugal input originating from the olfactory cortex (de Olmos et al., 1978; Haberly and Price, 1978), which could be sensitive to the state of the animal (Murakami et al., 2005). Taken together, our results suggest that wakefulness greatly enhances the impact of inhibitory circuits on olfactory bulb odor representations. We envision that the sparsening and richer temporal dynamics of mitral cell odor representations we observed in the awake state may be a result of shaping by active inhibitory circuits. It will be interesting to determine whether wakefulness also enhances the activity of interneurons in other brain regions.

Dynamic Experience-Dependent Plasticity

We showed that repeated brief odor experience leads to a modification of mitral cell activity that accumulates across days and persists for over a month. Hence, experience-dependent plasticity in the olfactory bulb is not just a transient adaptation to continuous odor stimuli, but rather a process that integrates months of odor experience. Odor experience does not lead to global changes in the responsiveness in the olfactory bulb, but rather its effect is highly odor specific, shifting the odor tuning of individual mitral cells away from experienced odors. This experience-specific tuning shift, in contrast to a general gain decrease, enables odor-specific plasticity in the olfactory bulb, where different odors are represented by overlapping ensembles of mitral cells. Additionally, this experience-dependent modulation represents a dynamic process, since it recovers and is repeatable with different odors.

An important feature of the experience-dependent plasticity described here is that the expression of the plasticity depends critically on wakefulness. Although previous studies have characterized the effects of odor experience on shorter timescales in anesthetized rodents (Buonviso and Chaput, 2000; Buonviso et al., 1998; Chaudhury et al., 2010; Fletcher and Wilson, 2003; Spors and Grinvald, 2002; Wilson, 2000; Wilson and Linster, 2008), our results reveal that olfactory bulb odor representations in awake mice are much more dynamic than previously shown in anesthetized animals. Previous literature suggests that prolonged odor stimulation (30 s to minutes) is required for short-term habituation in anesthetized animals (Chaudhury et al., 2010; Wilson, 2000; Wilson and Linster, 2008). In awake animals, even brief odor experience causes an odor-specific effect on mitral cell responses that lasts for several weeks; mitral cells respond more strongly to novel stimuli, and their "library" of familiar stimuli is constantly updated by recent experience. Even though our experiments were performed in the laboratory with a limited odor environment, animals in the wild live in odor environments that routinely change due to, for example, seasonal changes. Therefore, we speculate that mitral cell tuning properties of animals in their natural settings are also shaped by recent odor experience.

Implications on Odor Coding: Novel versus Familiar

We showed that mitral cell responses are more sparse and temporally dynamic in awake animals compared to anesthetized brain states. As a result of the sparsening and increased temporal dynamics, each mitral cell response in the awake state carries more information about odor identity. Experience further sparsens representations of familiar odors during wakefulness (Figure 8). We propose that this sparsening reduces the redundancy of the odor code, decreasing the metabolic load for representing frequently encountered stimuli. In contrast, novel or unfamiliar odors activate larger populations of mitral cells, which could serve as a "novelty detection" mechanism to alert the

animal of a change in the environment by representing unfamiliar stimuli with increased salience.

EXPERIMENTAL PROCEDURES

See Supplemental Experimental Procedures for detailed procedures. Briefly, for mitral cell imaging, AAV2/1-syn-FLEX-GCaMP3 was injected in the right olfactory bulb of PCdh21-Cre mice. For granule cell imaging, AAV2/1-syn-GCaMP3 or AAV2/1-syn-FLEX-GCaMP3 was injected in the right olfactory bulb of wild-type or GAD2-Cre mice, respectively. A custom headplate and chronic window were implanted and mice were head fixed under a two-photon microscope for in vivo imaging. Odors were applied for 4 s/trial with 1–2 min of intertrial intervals.

SUPPLEMENTAL INFORMATION

Supplemental Information includes eight figures and Supplemental Experimental Procedures and can be found with this article online at http://dx.doi.org/10.1016/j.neuron.2012.09.037.

ACKNOWLEDGMENTS

We thank S. Kalina, L. Xiao, I. Hsieh, and S. Moghadam for technical assistance, A. Peters and A. Mitani for help with data analysis, J. Moore for help with the sniff monitoring apparatus, Y. Yoshihara for the Tbx21 antibody, L.L. Looger, J. Akerboom, D.S. Kim, and the GECI Project at Janelia Farm Research Campus for making GCaMP available, and W. Kristan, R. Malinow, M. Scanziani, and members of the Komiyama laboratory for comments on the manuscript. This work was supported by grants from Japan Science and Technology Agency (PRESTO), NIH (P30, NS069301-01), Pew Charitable Trusts, Alfred P. Sloan Foundation, David & Lucile Packard Foundation, and New York Stem Cell Foundation to T.K., from NIH (R01, DC04682) to J.S.I., from NIH (R21, DC012641-01) to T.K. and J.S.I., and by NIH Training Grant (5T32GM007240) to M.W.C. T.K. is a NYSCF-Robertson Investigator.

Accepted: September 28, 2012
Published: December 5, 2012

REFERENCES

Adrian, E.D. (1950). The electrical activity of the mammalian olfactory bulb. Electroencephalogr. Clin. Neurophysiol. *2*, 377–388.

Arevian, A.C., Kapoor, V., and Urban, N.N. (2008). Activity-dependent gating of lateral inhibition in the mouse olfactory bulb. Nat. Neurosci. *11*, 80–87.

Atasoy, D., Aponte, Y., Su, H.H., and Sternson, S.M. (2008). A FLEX switch targets Channelrhodopsin-2 to multiple cell types for imaging and long-range circuit mapping. J. Neurosci. *28*, 7025–7030.

Bathellier, B., Buhl, D.L., Accolla, R., and Carleton, A. (2008). Dynamic ensemble odor coding in the mammalian olfactory bulb: sensory information at different timescales. Neuron *57*, 586–598.

Belluscio, L., and Katz, L.C. (2001). Symmetry, stereotypy, and topography of odorant representations in mouse olfactory bulbs. J. Neurosci. *21*, 2113–2122.

Bozza, T., McGann, J.P., Mombaerts, P., and Wachowiak, M. (2004). In vivo imaging of neuronal activity by targeted expression of a genetically encoded probe in the mouse. Neuron *42*, 9–21.

Buck, L., and Axel, R. (1991). A novel multigene family may encode odorant receptors: a molecular basis for odor recognition. Cell *65*, 175–187.

Buonviso, N., and Chaput, M. (2000). Olfactory experience decreases responsiveness of the olfactory bulb in the adult rat. Neuroscience *95*, 325–332.

Buonviso, N., Gervais, R., Chalansonnet, M., and Chaput, M. (1998). Short-lasting exposure to one odour decreases general reactivity in the olfactory bulb of adult rats. Eur. J. Neurosci. *10*, 2472–2475.

Cang, J., and Isaacson, J.S. (2003). In vivo whole-cell recording of odor-evoked synaptic transmission in the rat olfactory bulb. J. Neurosci. *23*, 4108–4116.

Carey, R.M., and Wachowiak, M. (2011). Effect of sniffing on the temporal structure of mitral/tufted cell output from the olfactory bulb. J. Neurosci. *31*, 10615–10626.

Chaudhury, D., Manella, L., Arellanos, A., Escanilla, O., Cleland, T.A., and Linster, C. (2010). Olfactory bulb habituation to odor stimuli. Behav. Neurosci. *124*, 490–499.

Cury, K.M., and Uchida, N. (2010). Robust odor coding via inhalation-coupled transient activity in the mammalian olfactory bulb. Neuron *68*, 570–585.

Davison, I.G., and Katz, L.C. (2007). Sparse and selective odor coding by mitral/tufted neurons in the main olfactory bulb. J. Neurosci. *27*, 2091–2101.

de Olmos, J., Hardy, H., and Heimer, L. (1978). The afferent connections of the main and the accessory olfactory bulb formations in the rat: an experimental HRP-study. J. Comp. Neurol. *181*, 213–244.

Dhawale, A.K., Hagiwara, A., Bhalla, U.S., Murthy, V.N., and Albeanu, D.F. (2010). Non-redundant odor coding by sister mitral cells revealed by light addressable glomeruli in the mouse. Nat. Neurosci. *13*, 1404–1412.

Dombeck, D.A., Khabbaz, A.N., Collman, F., Adelman, T.L., and Tank, D.W. (2007). Imaging large-scale neural activity with cellular resolution in awake, mobile mice. Neuron *56*, 43–57.

Doucette, W., and Restrepo, D. (2008). Profound context-dependent plasticity of mitral cell responses in olfactory bulb. PLoS Biol. *6*, e258.

Doucette, W., Gire, D.H., Whitesell, J., Carmean, V., Lucero, M.T., and Restrepo, D. (2011). Associative cortex features in the first olfactory brain relay station. Neuron *69*, 1176–1187.

Eyre, M.D., Antal, M., and Nusser, Z. (2008). Distinct deep short-axon cell subtypes of the main olfactory bulb provide novel intrabulbar and extrabulbar GABAergic connections. J. Neurosci. *28*, 8217–8229.

Fantana, A.L., Soucy, E.R., and Meister, M. (2008). Rat olfactory bulb mitral cells receive sparse glomerular inputs. Neuron *59*, 802–814.

Fletcher, M.L., and Wilson, D.A. (2003). Olfactory bulb mitral-tufted cell plasticity: odorant-specific tuning reflects previous odorant exposure. J. Neurosci. *23*, 6946–6955.

Friedrich, R.W., and Laurent, G. (2001). Dynamic optimization of odor representations by slow temporal patterning of mitral cell activity. Science *291*, 889–894.

Friedrich, R.W., Habermann, C.J., and Laurent, G. (2004). Multiplexing using synchrony in the zebrafish olfactory bulb. Nat. Neurosci. *7*, 862–871.

Haberly, L.B., and Price, J.L. (1978). Association and commissural fiber systems of the olfactory cortex of the rat. J. Comp. Neurol. *178*, 711–740.

Holtmaat, A., Bonhoeffer, T., Chow, D.K., Chuckowree, J., De Paola, V., Hofer, S.B., Hübener, M., Keck, T., Knott, G., Lee, W.C., et al. (2009). Long-term, high-resolution imaging in the mouse neocortex through a chronic cranial window. Nat. Protoc. *4*, 1128–1144.

Igarashi, K.M., and Mori, K. (2005). Spatial representation of hydrocarbon odorants in the ventrolateral zones of the rat olfactory bulb. J. Neurophysiol. *93*, 1007–1019.

Isaacson, J.S., and Strowbridge, B.W. (1998). Olfactory reciprocal synapses: dendritic signaling in the CNS. Neuron *20*, 749–761.

Johnson, B.A., Farahbod, H., Saber, S., and Leon, M. (2005). Effects of functional group position on spatial representations of aliphatic odorants in the rat olfactory bulb. J. Comp. Neurol. *483*, 192–204.

Kay, L.M., and Laurent, G. (1999). Odor- and context-dependent modulation of mitral cell activity in behaving rats. Nat. Neurosci. *2*, 1003–1009.

Komiyama, T., Sato, T.R., O'Connor, D.H., Zhang, Y.X., Huber, D., Hooks, B.M., Gabitto, M., and Svoboda, K. (2010). Learning-related fine-scale specificity imaged in motor cortex circuits of behaving mice. Nature *464*, 1182–1186.

Laurent, G., Wehr, M., and Davidowitz, H. (1996). Temporal representations of odors in an olfactory network. J. Neurosci. *16*, 3837–3847.

Mazor, O., and Laurent, G. (2005). Transient dynamics versus fixed points in odor representations by locust antennal lobe projection neurons. Neuron *48*, 661–673.

Meredith, M. (1986). Patterned response to odor in mammalian olfactory bulb: the influence of intensity. J. Neurophysiol. *56*, 572–597.

Mombaerts, P., Wang, F., Dulac, C., Chao, S.K., Nemes, A., Mendelsohn, M., Edmondson, J., and Axel, R. (1996). Visualizing an olfactory sensory map. Cell *87*, 675–686.

Mori, K., Mataga, N., and Imamura, K. (1992). Differential specificities of single mitral cells in rabbit olfactory bulb for a homologous series of fatty acid odor molecules. J. Neurophysiol. *67*, 786–789.

Murakami, M., Kashiwadani, H., Kirino, Y., and Mori, K. (2005). State-dependent sensory gating in olfactory cortex. Neuron *46*, 285–296.

Nagai, Y., Sano, H., and Yokoi, M. (2005). Transgenic expression of Cre recombinase in mitral/tufted cells of the olfactory bulb. Genesis *43*, 12–16.

Nicoll, R.A. (1972). The effects of anaesthetics on synaptic excitation and inhibition in the olfactory bulb. J. Physiol. *223*, 803–814.

Onoda, N. (1992). Odor-induced fos-like immunoreactivity in the rat olfactory bulb. Neurosci. Lett. *137*, 157–160.

Pressler, R.T., and Strowbridge, B.W. (2006). Blanes cells mediate persistent feedforward inhibition onto granule cells in the olfactory bulb. Neuron *49*, 889–904.

Rinberg, D., Koulakov, A., and Gelperin, A. (2006a). Sparse odor coding in awake behaving mice. J. Neurosci. *26*, 8857–8865.

Rinberg, D., Koulakov, A., and Gelperin, A. (2006b). Speed-accuracy tradeoff in olfaction. Neuron *51*, 351–358.

Rubin, B.D., and Katz, L.C. (1999). Optical imaging of odorant representations in the mammalian olfactory bulb. Neuron *23*, 499–511.

Schoppa, N.E., and Urban, N.N. (2003). Dendritic processing within olfactory bulb circuits. Trends Neurosci. *26*, 501–506.

Schoppa, N.E., Kinzie, J.M., Sahara, Y., Segerson, T.P., and Westbrook, G.L. (1998). Dendrodendritic inhibition in the olfactory bulb is driven by NMDA receptors. J. Neurosci. *18*, 6790–6802.

Shepherd, G.M., Chen, W.R., and Greer, C.A. (2004). Olfactory bulb. In The Synaptic Organization of the Brain, G.M. Shepherd, ed. (New York: Oxford University Press), pp. 165–216.

Shusterman, R., Smear, M.C., Koulakov, A.A., and Rinberg, D. (2011). Precise olfactory responses tile the sniff cycle. Nat. Neurosci. *14*, 1039–1044.

Soucy, E.R., Albeanu, D.F., Fantana, A.L., Murthy, V.N., and Meister, M. (2009). Precision and diversity in an odor map on the olfactory bulb. Nat. Neurosci. *12*, 210–220.

Spors, H., and Grinvald, A. (2002). Spatio-temporal dynamics of odor representations in the mammalian olfactory bulb. Neuron *34*, 301–315.

Stewart, W.B., and Scott, J.W. (1976). Anesthetic-dependent field potential interactions in the olfactory bulb. Brain Res. *103*, 487–499.

Stewart, W.B., Kauer, J.S., and Shepherd, G.M. (1979). Functional organization of rat olfactory bulb analysed by the 2-deoxyglucose method. J. Comp. Neurol. *185*, 715–734.

Stopfer, M., Bhagavan, S., Smith, B.H., and Laurent, G. (1997). Impaired odour discrimination on desynchronization of odour-encoding neural assemblies. Nature *390*, 70–74.

Tan, J., Savigner, A., Ma, M., and Luo, M. (2010). Odor information processing by the olfactory bulb analyzed in gene-targeted mice. Neuron *65*, 912–926.

Tian, L., Hires, S.A., Mao, T., Huber, D., Chiappe, M.E., Chalasani, S.H., Petreanu, L., Akerboom, J., McKinney, S.A., Schreiter, E.R., et al. (2009). Imaging neural activity in worms, flies and mice with improved GCaMP calcium indicators. Nat. Methods *6*, 875–881.

Tsuno, Y., Kashiwadani, H., and Mori, K. (2008). Behavioral state regulation of dendrodendritic synaptic inhibition in the olfactory bulb. J. Neurosci. *28*, 9227–9238.

Urban, N.N., and Arevian, A.C. (2009). Computing with dendrodendritic synapses in the olfactory bulb. Ann. N Y Acad. Sci. *1170*, 264–269.

Verhagen, J.V., Wesson, D.W., Netoff, T.I., White, J.A., and Wachowiak, M. (2007). Sniffing controls an adaptive filter of sensory input to the olfactory bulb. Nat. Neurosci. *10*, 631–639.

Wachowiak, M., and Cohen, L.B. (2001). Representation of odorants by receptor neuron input to the mouse olfactory bulb. Neuron *32*, 723–735.

Wilson, D.A. (2000). Comparison of odor receptive field plasticity in the rat olfactory bulb and anterior piriform cortex. J. Neurophysiol. *84*, 3036–3042.

Wilson, D.A., and Linster, C. (2008). Neurobiology of a simple memory. J. Neurophysiol. *100*, 2–7.

Wilson, R.I., and Mainen, Z.F. (2006). Early events in olfactory processing. Annu. Rev. Neurosci. *29*, 163–201.

Xu, F., Greer, C.A., and Shepherd, G.M. (2000). Odor maps in the olfactory bulb. J. Comp. Neurol. *422*, 489–495.

Xu, F., Liu, N., Kida, I., Rothman, D.L., Hyder, F., and Shepherd, G.M. (2003). Odor maps of aldehydes and esters revealed by functional MRI in the glomerular layer of the mouse olfactory bulb. Proc. Natl. Acad. Sci. USA *100*, 11029–11034.

Yang, X., Renken, R., Hyder, F., Siddeek, M., Greer, C.A., Shepherd, G.M., and Shulman, R.G. (1998). Dynamic mapping at the laminar level of odor-elicited responses in rat olfactory bulb by functional MRI. Proc. Natl. Acad. Sci. USA *95*, 7715–7720.

Yokoi, M., Mori, K., and Nakanishi, S. (1995). Refinement of odor molecule tuning by dendrodendritic synaptic inhibition in the olfactory bulb. Proc. Natl. Acad. Sci. USA *92*, 3371–3375.

Yoshihara, S., Omichi, K., Yanazawa, M., Kitamura, K., and Yoshihara, Y. (2005). Arx homeobox gene is essential for development of mouse olfactory system. Development *132*, 751–762.